

Chapter 2 Mechanical and Dynamic Behavior of Rock Masses

2.1 Overview of Rock Masses

2.1.1 Rock material and rock masses

Natural rock that differs from most other engineering materials consists of rock material and a lot of discontinuities (Fig. 2.1). A clear distinction must be made between the rock material and the rock masses. Rock material is the term used to describe the intact rock between discontinuities and the rock masses is the total in situ medium containing discontinuities. In the engineering view, rock material can be treated to be uniform with high stiffness and has relatively high strength and small deformability. However, the discontinuities produce most of the deformations in rock masses and have a dominant effect on the response of the rock masses to the rock cavern (Brady and Brown 1993). In the case of wave propagation induced by dynamic loads, the discontinuities give more attenuation than rock material to the wave propagation. Wave transmission, reflection and energy absorption will occur when the wave hits a discontinuity (Cook 1992).



Figure 2.1. Typical jointed rock masses

2.1.2 Major types of discontinuities

Discontinuities in a rock mass were formed under different geological conditions and have undergone a long geological history. According to their formation and geological characteristics, they can be classified into three types: rock interface, joint and fault.

Rock interface was originally formed together with the formation of rocks. A typical rock interface is the bedding plane existing in the sedimentary rocks. It divides sedimentary rocks into beds or strata and represents interruptions in the course of deposition of the rock masses. It is often perfectly-bonded between two opposite sides. Both compression and tension can be transmitted across the interface, and no sliding displacement occurs. The interface is actually a discontinuity of media properties and makes the rock masses stratified anisotropic medium.

Joints are the most common and generally the most significant discontinuities in the rock masses. Joints are breaks of geological origin along which there has been no visible displacement. Joints may be saturated or filled with other materials. They can be considered as imperfectly-bonded interfaces in which tension cannot be transmitted and sliding displacements may occur. Joints are displacement discontinuities and lead the rock masses to be a fractured or jointed medium.

Faults are fractures on which identifiable shear displacement takes place. They may be recognised by the relative displacement of the rock on opposite sides of the fault plane and may have a wide fractured or squeezing zone due to the strong geological activities.

As commonly done in rock mechanics, in this context, the term “joint” is used to represent a collective term for all discontinuities in rock masses.

2.1.3 Important geomechanical properties of joints

The mechanical behavior of joints is governed by their geomechanical properties including orientation, spacing, persistence, aperture, filling, roughness and matching (Brady and Brown 1993).

Orientation is described by the dip of the line of maximum declination on the joint surface measured from the horizontal, and the dip direction or azimuth of this line, measured clockwise from true north. The orientations of joints relative to the faces of excavations have a dominant effect on the potential instability due to falls of blocks of rock or slip on the joints. The mutual orientations of joints will determine the shapes of the blocks into which the rock masses are divided.

Spacing is the perpendicular distance between adjacent joints, and is usually expressed as the mean spacing of a particular set of joints. The spacing of joints with their connectivity and dimension together determines the sizes of the blocks making up the rock masses. The mechanism of deformation and failure can vary with the ratio of joint spacing to excavation size. Engineering properties such as cavability, fragmentation characteristics and rock masses permeability also vary with joint spacing.

Persistence is the term used to describe the area extent or size of a joint within a plane. It can be crudely quantified by observing the trace lengths of joints on exposed surfaces. It is one of the most important rock masses parameters but one of the most difficult to determine. The persistence of joints will have a major influence on the shear strength developed in the plane of the joint and on the

fragmentation characteristics, cavability and permeability of the rock masses.

Aperture is the perpendicular distance separating the adjacent rock walls of an open joint in which the intervening space is filled with air or water. Aperture is thereby distinguished from the width of a filled joint. The aperture and its area variation have an influence on the shear strength of the joint and specially on the permeability or hydraulic conductivity of the joint and of the rock masses.

Filling is the term used to describe material separating the adjacent rock wall of joints. Filling materials have a major influence on the shear strength of joints.

Roughness is a measure of the inherent surface unevenness and waviness of the joint relative to its mean plane. The wall roughness of a joint has a potentially important influence on its shear strength, especially in the case of undisplaced and interlocked features. The importance of roughness declines with increasing aperture, filling thickness or previous shear displacement. Barton (1971; 1973 & 1976) proposed a joint roughness coefficient (JRC) to describe the surface roughness scaled from zero to 20. Typical roughness profiles and corresponding range of JRC for 20 cm (JRC₂₀) and 100 cm (JRC₁₀₀) samples are shown in Figure 2.2

Matching is proposed as an independent joint surface geometrical parameter. The joint matching coefficient (JMC) represents the percentage of joint surfaces in contact (Zhao 1997a). Figure 2.3 shows the classification of the JMC of a joint. The JMC is often coupled with the existing joint roughness coefficient (JRC) to fully describe the geometrical properties and to assess the hydromechanical behavior of joints. It has been demonstrated that the JMC is an important factor governing the aperture, normal close, stiffness, shear strength and hydraulic conductivity of the joints.


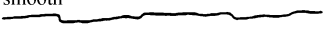
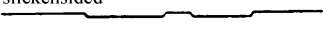

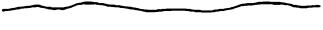
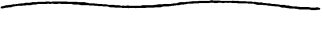


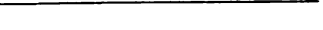
Description of Joint Types		JRC ₂₀	JRC ₁₀₀
Stepped			
I	rough 	20	11
II	smooth 	14	9
III	slickensided 	11	8
Undulating			
IV	rough 	14	9
V	smooth 	11	8
VI	slickensided 	7	6
Planar			
VII	rough 	2.5	2.3
VIII	smooth 	1.5	0.9
IX	slickensided 	0.5	0.4

Figure 2.2. Typical roughness profiles and corresponding range of JRC (after Barton and Bandis 1990)

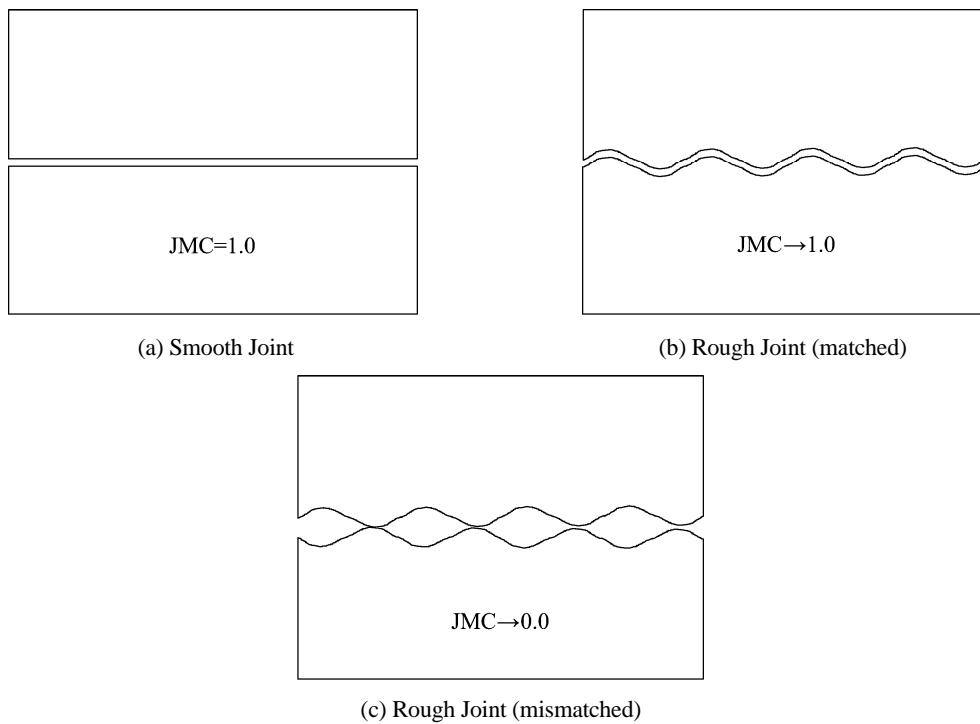


Figure 2.3. Classification of JMC (after Zhao 1997a)

2.2 Mechanical Behavior of Jointed Rock Masses

2.2.1 Rock material behavior

Rock material can have compression as well as considerable tensile strength depending on the rock type. The tensile strength of rock material is often much lower than the compressive strength (less than one-tenth, generally), so the main concern in rock material is the characteristic under compression loading, which includes stress-strain relationship and compressive strength.

2.2.1.1 Stress-strain relationship under compression

Similar to other geomaterials, e.g., soil and concrete, a rock material has two types of stress-strain relationship under compression load. They are brittle and ductile. Uniaxial and multipleaxial tests (including biaxial, triaxial and polyaxial tests) are often used to determine the stress-strain relation of rock material.

Figure 2.4 shows a typical stress-strain relation of rock material under uniaxial compression. It starts with a linear deformation and is followed by a plastic deformation until the peak strength. The curve then drops down gradually and tends to be flat (residual strength). The deformation modulus can also be determined from the stress-strain relation.

Figure 2.5 shows the axial stress-axial strain curves at various confining stresses. It can be seen that the strengths (peak and residual) increase with increasing confining stress. With the increase of confining stress, the stress-strain relation of rock material may be transited from brittle to ductile.

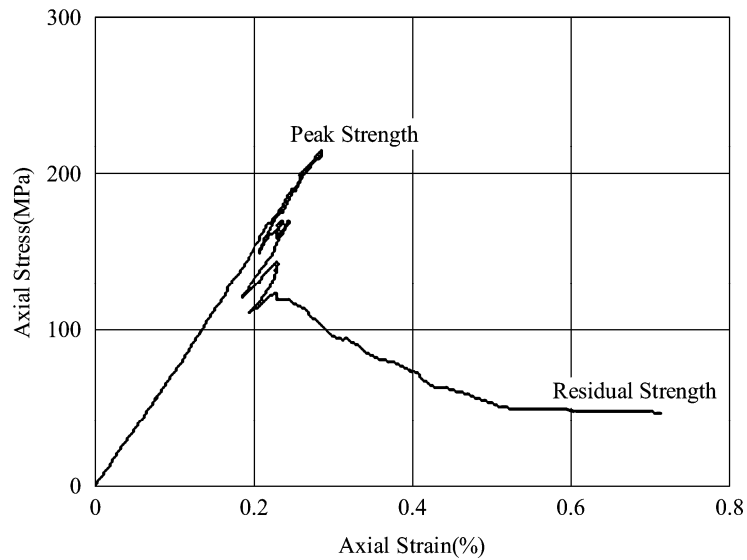


Figure 2.4. Typical stress-strain relation of rock material under axial compression (after Zhao *et al.* 1996)

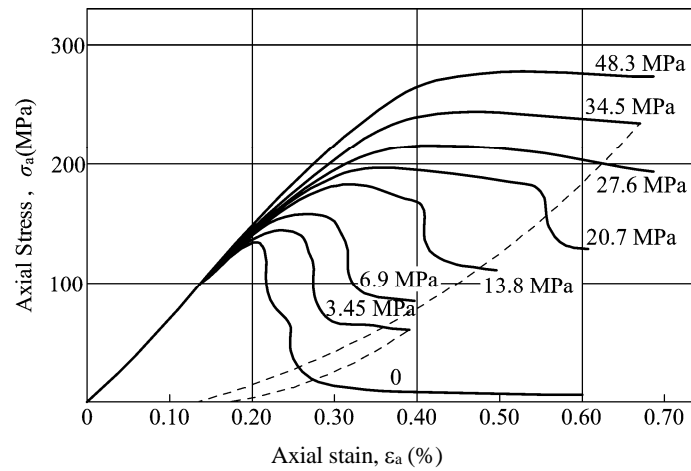


Figure 2.5. Stress-strain relation of rock material at various confining stresses (after Brady and Brown 1993)

2.2.1.2 Compressive strength criteria

Various strength criteria have been proposed to estimate the strength (peak or residual) of rock material.

Coulomb shear strength criterion

The Coulomb shear strength criterion is widely used in numerical modeling of rock material and rock masses, which is expressed as

$$\tau = c + \sigma_n \tan \phi \quad (2.1)$$

where c is the cohesion and ϕ is the friction angle.

The uniaxial compressive strength σ_c and tensile strength σ_T can be derived from Equation (2.1):

$$\sigma_c = \frac{2c \cos \phi}{1 - \sin \phi}, \quad \sigma_T = \frac{2c \cos \phi}{1 + \sin \phi} \quad (2.2)$$

Hoek-Brown Criterion

Hoek and Brown (1980) proposed a peak triaxial compressive strength criterion of isotropic rock material as

$$\frac{\sigma_1}{\sigma_c} = \frac{\sigma_3}{\sigma_c} + \left(m \frac{\sigma_3}{\sigma_c} + 1.0 \right)^{1/2} \quad (2.3)$$

where m is a constant varying with rock type.

2.2.2 Rock joint behavior

The mechanical behavior of a joint is often expressed by the normal stress-deformation, shear stress-deformation and dilation as shown in Figure 2.6, where k_n and k_s represent the normal stiffness and shear stiffness, respectively. They can be written as

$$k_n = \frac{\Delta \sigma_n}{\Delta \delta_n}, \quad k_s = \frac{\Delta \tau}{\Delta \delta_s} \quad (2.4)$$

where Δ denotes an increment, σ_n , δ_n , τ and δ_s are normal stress, normal deformation, shear stress and shear deformation, respectively.

The joint can be compressed but not failed. However, the joint has a tensile strength. When the tensile strength is exceeded, the tensile resistance will be zero. In most cases, the tensile strength is very low and thus often assumed as zero. The joint has a limiting resistance against shear load. When the peak shear strength is exceeded, the slip will occur at the joint. But the joint still has residual shear strength.

The joint constitutive model is very important to estimate the joint mechanical behavior and must be provided to numerical modeling, including the normal stress-deformation relation, shear stress-deformation relation and shear strength criteria. Various models of them have been proposed.

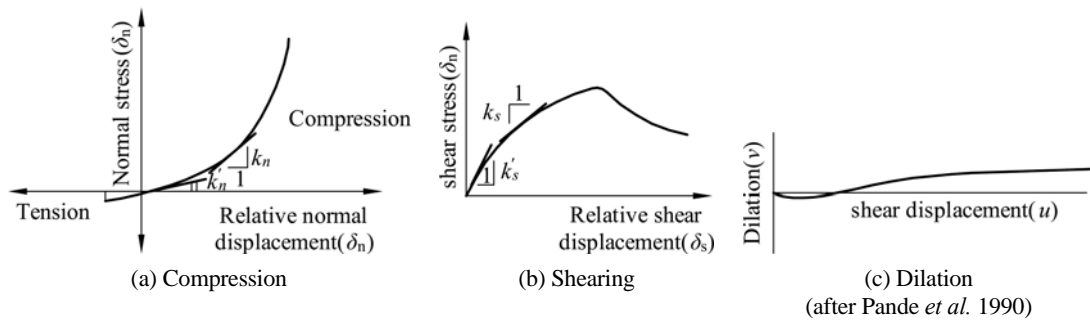


Figure 2.6. Mechanical Behavior of a Joint

2.2.2.1 Normal stress-deformation relation

Goodman model

For the normal stress-deformation relation of rock joints, Goodman *et al.* (1968) proposed a hyperbolic model given by

$$\sigma_n = \frac{\delta_n \sigma_i}{\delta_{nm} - \delta_n} + \sigma_i \quad (2.5)$$

where σ_n is the normal stress; δ_n is the normal closure; σ_i is the initial stress level and δ_{nm} is the maximum closure of the joint.

Goodman (1976) suggested an alternative version of equation (2.5) as

$$\frac{\sigma_n - \sigma_i}{\sigma_i} = a \left(\frac{\delta_n}{\delta_{nm} - \delta_n} \right)^b \quad (2.6)$$

where a and b are two material constants.

Kulhaway Model

Another hyperbolic model was presented by Kulhaway (1975) to fit the stress-strain curve of a rock joint under triaxial compression with basic form:

$$\sigma = \frac{\varepsilon}{a + b\varepsilon} \quad (2.7)$$

where σ is the deviator stress; ε is the axial strain; a and b are constants.

Bandis Model

Based on a series of laboratory tests, Bandis (1980) proposed a hyperbolic model with a similar form to the Kulhaway model, to describe the normal stress-displacement behavior of a rock joint (Bandis *et al.* 1983):

$$\sigma_n = \frac{\delta_n k_{ni} \delta_{nm}}{\delta_{nm} - \delta_n} \quad (2.8)$$

where k_{ni} in MPa is initial normal stiffness which is calculated by:

$$k_{ni} = 0.0178 \left[\frac{JCS}{A_{jn}} \right] + 1.748JRC - 7.155 \quad (2.9)$$

where A_{jn} is the joint aperture in millimeter at zero normal stress; JRC is the joint roughness coefficient and JCS is the laboratory-scale joint wall compressive strength. The allowable closure δ_{nm} for load i is given by:

$$\delta_{nm} = a_i + b_i JRC + c_i \left[\frac{JCS}{A_{jn}} \right]^{d_i} \quad (2.10)$$

where a_i , b_i , c_i , d_i are constants associated with load cycle number.

Brown and Scholz Model

Brown and Scholz (1986) proposed a logarithmic function to present the normal behavior of rock joints:

$$\delta_n = c + b \ln(\sigma_n), \quad k_n = \sigma_n / b \quad (2.11)$$

where c and b are material constants determined by the geometry of the roughness profile.

Saeb and Amadei Model

After Bandis model, Saeb and Amadei (1992) proposed a normal model by considering the joint dilatancy:

$$\Delta\sigma_n = k_{nn}\Delta\delta_n + k_{ns}\Delta\delta_s \quad (2.12)$$

where k_{nn} and k_{ns} are two normal stiffness; Δ denotes an increment; δ_n and δ_s are joint normal closure and shear displacement, respectively.

Continuously-yielding Model

In the continuously-yielding model proposed by Cundall and Hart (1985), the response to normal loading is non-linear and expressed incrementally as

$$\Delta\sigma_n = k_n\Delta\delta_n \quad (2.13)$$

where the normal stiffness k_n is given by

$$k_n = a_n\sigma_n^{e_n} \quad (2.14)$$

representing the observed increase of stiffness with normal stress, where a_n and e_n are model parameters.

2.2.2.2 Shear stress-deformation relation

Kulhaway Model

A hyperbolic function was proposed by Kulhaway (1975) to express the non-linear behavior of a sheared joint in the pre-peak range:

$$\tau = \frac{\delta_s}{a + b\delta_s} \quad (2.15)$$

where δ_s is the shear displacement at a level of shear stress τ ; a is the constant representing the reciprocal of the initial stiffness and b is the constant representing the reciprocal of the horizontal asymptote to the τ - δ_s curve.

Goodman Model

The shear response of a joint to shear loading under constant normal stress is idealised by Goodman (1976), which consists of pre-peak, post-peak and residual regions. The model can be expressed as

$$\left. \begin{aligned} \tau &= k_s\delta_s \text{ with } k_s = \frac{\tau_p}{\delta_{sp}} \quad (\text{if } d_s < d_{sp}) \\ \tau &= \left(\frac{\tau_p - \tau_r}{\delta_{sp} - \delta_{sr}} \right) \delta_s + \left(\frac{\tau_r\delta_{sp} - \tau_p\delta_{sr}}{\delta_{sp} - \delta_{sr}} \right) \quad (\text{if } \delta_{sp} \leq \delta_s \leq \delta_{sr}) \\ \tau &= \tau_r \quad (\text{if } d_s > d_{sr}) \end{aligned} \right\} \quad (2.16)$$

where τ_p and δ_{sp} are the peak shear strength and displacement, respectively. Likewise, τ_r and δ_{sr} are the residual shear strength and displacement, respectively.

Saeb and Amadei Model

After Goodman model, Saeb and Amadei (1992) proposed a shear model by considering the joint dilatancy.

$$\tau = k_{sn} \Delta \delta_n + k_{ss} \Delta \delta_s \quad (2.17)$$

where k_{sn} and k_{ss} are two shear stiffness coefficients. Souley *et al.* (1995) presented an extension of the Saeb and Amadei model to take account of the effect of cyclic loading on joint normal and shear behavior.

2.2.2.3 Shear strength criteria

When a joint in rock masses is compressed under normal loading, a maximum closure and no tension are allowed. The joint peak shear strength is defined to be the peak value of shear stress as shown in Figure 2.6 (b). If the shear strength is exceeded, the joint will slip along the joint surface. During the slipping, the joint has still a resistance to the shear, which is so-called residual strength.

There are several criteria in estimating the joint shear strengths.

Coulomb Slip Model

The Coulomb slip criteria is often used to judge the shear failure of a joint.

$$\tau = c + \sigma_n \tan \phi \quad (2.18)$$

where c is the cohesion of the joint which is very small and often neglected; ϕ is the frictional angle of the joint.

Dilatant Model

The Coulomb slip criteria is derived by assuming the joint be smooth and clean. By testing artificial rough joints at low normal stresses, it was found that the shearing occurs by the riding over of asperities, which remain unbroken. The shear strength increases with normal stress linearly described by the dilatant model (Patton 1966; Withers 1964)

$$\tau = \sigma_n \tan(\phi + \phi_i) \quad (2.19)$$

where ϕ_i is the peak dilation angle.

JRC-JCS Model

The empirical JRC-JCS joint model, proposed by Barton and his co-workers (Barton 1971, 1973 & 1976; Barton and Choubey 1977; Barton *et al.* 1985; Barton and Bandis 1990; Bandis *et al.* 1981 & 1983), is the most commonly used shear strength criterion in rock mechanics and is expressed as

$$\tau = \sigma_n \tan[JRC \times \log_{10}(JCS / \sigma_n) + \phi_r] \quad (2.20)$$

where JRC is the joint roughness coefficient; JCS is the laboratory-scale joint wall compressive strength and ϕ_r is the basic friction angle of fresh unweathered joint in the range 28.5° to 31.5°.

JRC-JMC Model

The JRC-JCS shear strength model was initially based on artificial or fresh tension joints in artificial material and weak rocks, which, in general, represent rough and closely matched surfaces. However, it is found to overpredict the shear strength of natural joints in rocks. This is because the natural joints are often altered since the fracturing and the surfaces of joints are no longer closely matched.

Based on the laboratory tests of freshly induced joints and natural joints, Zhao (1997a) proposed the joint matching coefficient (JMC), an independent geomaterial parameter, to account for the degree of matching of the two joint surfaces. The JMC has a value scaled from zero to one, based on the percentage of joint surface area in contact relatively to the total joint surface area. Zhao (1997b) also proposed the JRC-JMC shear strength model by combining the JMC into the JRC-JCS model as

$$\tau = \sigma_n \tan[JRC \times JMC \times \log_{10}(JCS / \sigma_n) + \phi_r] \quad (2.21)$$

This model is implemented into the discrete element code UDEC by the author.

Jing et al. Model

Based on a series of laboratory tests under 3-D loading conditions, Jing *et al.* (1992) proposed a joint shear strength model as:

$$\tau = \sigma_n \tan[\phi_r + \phi_o (1 - \sigma_n / \sigma_c)^b] \quad (2.22)$$

where ϕ_o is the initial friction angle; ϕ_r is the residual friction angle; b is a material parameter representing the crushing effects of the asperity angle with respect to the normal stress; σ_c is the uniaxial compressive strength of the rock material.

Continuously-yielding Model

The continuously-yielding shear strength model was proposed by Cundall and Hart (1985) and revised by Lemos (1987). It provides a unified simulation of joint behavior, by taking account of continuous attrition of joint roughness with shear displacement. This is intended to simulate, in a simple fashion, the internal mechanism of progressive damage of the joint. A component of plastic deformation was introduced in the continuously-yielding shear model and attended all shear displacement, and progressive reduction of joint roughness and dilatancy with joint plastic deformation. The model displays irreversible, non-linear behavior from the onset of shearing. The shear stress increment is calculated as:

$$\Delta\tau = F \times k_s \times \Delta\delta_s \quad (2.23)$$

where F is a factor representing the tangent modulus relating to the joint roughness which depends on the distance from the actual stress to a defined bounding strength curve.

2.2.3 Rock mass behavior

Actual rock masses are often fractured by a lot of joints and become anisotropic media.

Therefore, the global response of the jointed rock masses is more concerned in rock engineering. Both rock material and joints in a rock mass generate the deformation and the failure of the rock mass depends on the stress distribution and joint mechanical properties. Figure 2.7 shows the failure of rock specimen containing a joint under triaxial compression and indicates that the rock failure depends on the inclination angle of the joint.

In the case of a rock containing several joint sets, the lowest strength envelope to the individual strength curves gives the overall strength as shown in Figure 2.8. When the rock is heavily jointed, it is often simply treated to be an equivalent continuous medium having material properties combined from rock material and joint properties (Hoek and Brown 1980).

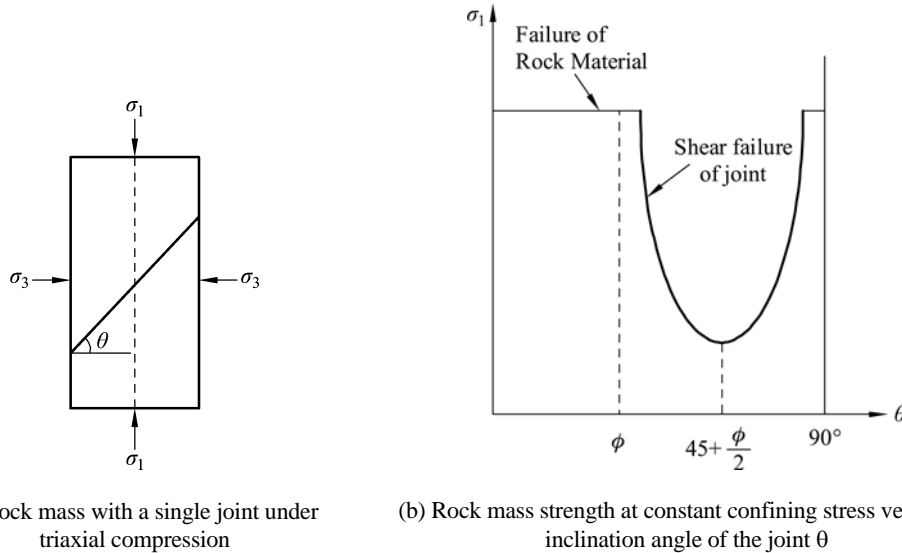
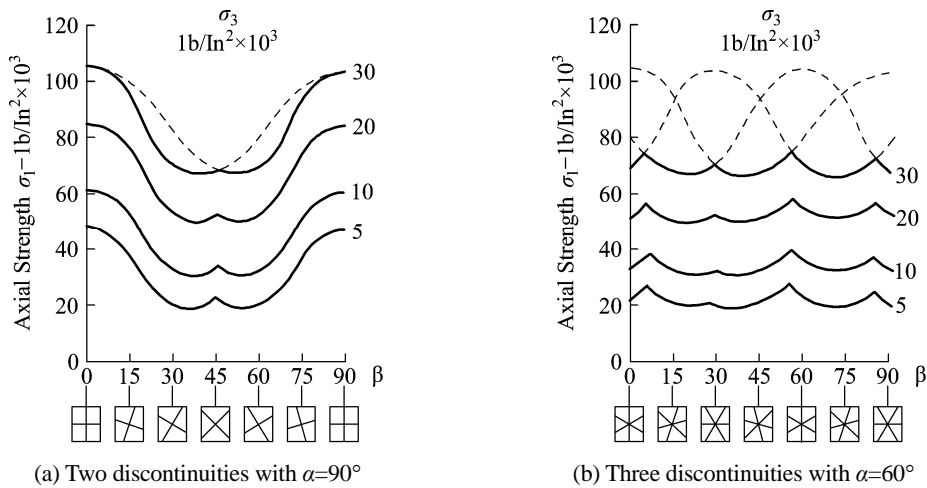
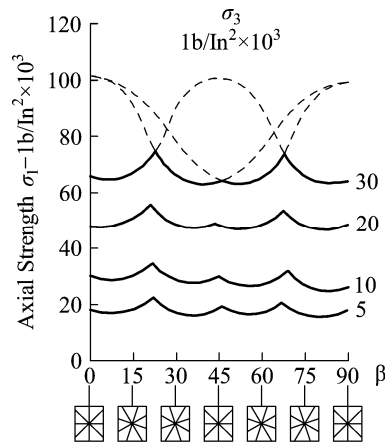


Figure 2.7. Compressive strength of rock masses with a single joint depending on the inclination angle of the joint (after Hoek and Brown 1980)





(c) Four discontinuities with $\alpha=45^\circ$

Figure 2.8. Strength curves for rock specimens with several joint sets (after Hoek and Brown 1980)

2.3 Dynamic Response of Jointed Rock Masses

The rock masses response to dynamic loads is more complicated than that to static loads depending on the loading rate.

2.3.1 Rock material response

Similar to other continuous materials, rock material provides geometric damping and material damping to the wave propagation. The wave subject to geometric spreading decreases in amplitude and frequency with distance from the wave source as the energy is distributed over an expanding surface. During the wave propagation, the wave energy dissipates in the host medium of rock material, due to the temperature exchange with surrounding media and deformation on the populated microcracks in rock material.

The dynamic behavior of rock material is often described by its strength (compression and tension strength), deformation modulus and stress-strain relationship, and mostly influenced by strain rate. Generally, the strength of rock material increases with increasing strain rate, but amount of increment varies with the rock types. Brace and Jones (1971) summarised the experimental results under different kinds of strain rate performed by other researchers. It is shown that the strengths of igneous rocks increases about 10% with the strain rate increasing of three order of magnitude (10^3 s^{-1}), while the strengths of limestone increase 18%. Kumar (1968) found that the strength of rock is related to the velocity of propagation and the total number of micro-cracks. The increase of strain rate may induce the increase in number and propagation velocity of micro-cracks. This is why the increase of strain rate induces the increase of rock strength. Zhao and Zhao (1998) reviewed the experimental results on rock strength at different strain rates and found that rock strength increases with increasing strain rate. The increasing rate of the rock strength with increasing strain rate depends primarily on rock type, the existence of micro-cracks and the porosity of rock. Rocks of high strength are less

sensitive to the strain rate effect. In some cases, a sudden increase in compressive strength can occur at high strain rate. A schematic relation between compressive strength and strain rate was suggested by Zhao and Zhao (1998) as shown in Figure 2.9. It was also found that the elastic modulus increases with the increase in strain rate (Yang and Li 1992). As a general rule, dynamic modulus may be greater than static modulus by up to 300%. The difference between them is usually ascribed to the effects of closed cracks on deformation (Brady 1993).

2.3.2 Joint response

It is commonly accepted that the joints in rock masses dominate the response of jointed rock masses under static loading (Goodman 1976; Bandis et al. 1983). However, relatively few studies on the wave propagation through jointed rock masses have been conducted either theoretically or experimentally. Swolfs *et al.* (1981) conducted a field test on a 2 m³ of sandstone block containing a near-vertical joint and observed a 40% decrease in seismic velocity due to the in situ stresses unloading of the block. King *et al.* (1984) measured the amplitudes and travel times of high-frequency seismic waves propagated parallel and perpendicular to joints in basalt. He found that lower velocities and more high-frequency attenuation are obtained in the direction perpendicular to the joints than in the direction parallel to them.

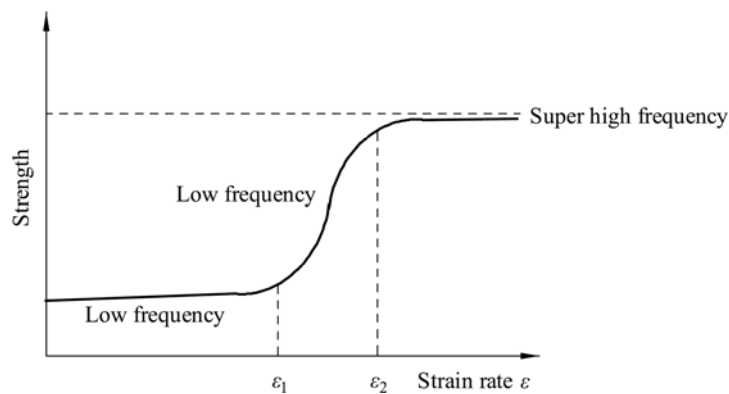


Figure 2.9. Schematic relation between compressive strength and strain rate (after Zhao and Zhao 1998)

2.3.2.1 Wave transmission and reflection at joints

When an incident wave hits a jointed interface, the reflection and transmission waves will occur as shown in Figure 2-10 (Cook 1992). In Figure 2.10, P is compression wave, S_v , and S_h are plane shear waves polarised in the x - z plane and the x - y plane, respectively. ϕ_i and θ_i ($i=1, 2$) are incident, transmitted or reflected angles. Only material damping is considered and represented by the transmission coefficient, reflection coefficient and energy absorption coefficient. The geometric damping is often neglected because the thickness of joints is too small relative to the model size.

Kendall and Tabor (1971) found that when a seismic wave goes through a joint in rock masses,

seismic stresses are continuous but displacements are not. They derived a solution of the transmission and reflection of compression waves normal to the plane of a joint. Their results showed that both the amplitude and phase of these waves depend upon the ratio of joint stiffness to the seismic impedance of the material, and on the frequency of the wave.

Extensive laboratory experiments on seismic wave transmission across natural joints in laboratory samples were conducted by Pyrak-Nolte (1988). It was shown that a joint can be described either as a displacement discontinuity, if the coupling between the two half spaces is an elastic stiffness, or as a velocity discontinuity, if the coupling is viscous. In the case of a displacement discontinuity, both the amplitude and phase of reflected, transmitted and converted waves depend upon the ratio of stiffness to seismic impedance and on the frequency. For a pure velocity discontinuity, the amplitudes of reflected, transmitted and converted wave depend only upon the ratio of viscosity to seismic impedance. Natural joints may be expected to comprise both a displacement discontinuity and a velocity discontinuity possessing elastic as well as viscous coupling across the interface. Pyrak-Nolte (1988) derived complete solutions for all angles of incidence and different seismic impedance in each half space.

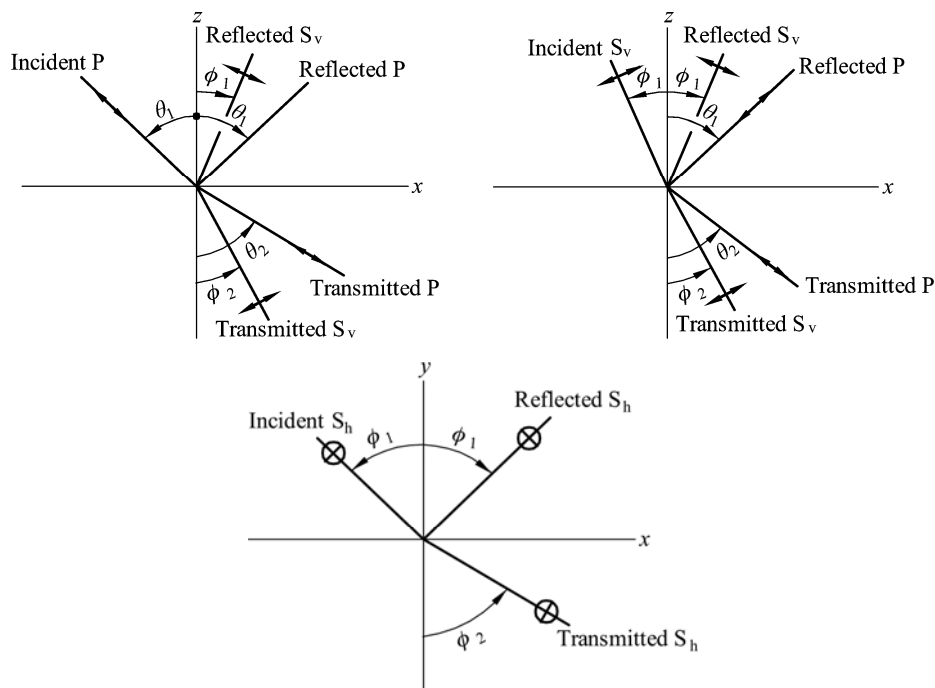


Figure 2.10. Wave transmission and reflection at a rock joint (after Cook 1992)

Majer *et al.* (1990) investigated the effect of a single joint on the transmitted waveform and corresponding amplitude spectra, and found that the transmitted wave is slowed and attenuated with decreasing joint stiffness. The attenuation is characterized by both decreasing amplitude and filtering of the high frequency components of the pulse as shown in Figure 2.11, where k denotes the joint stiffness and z is the wave impedance.

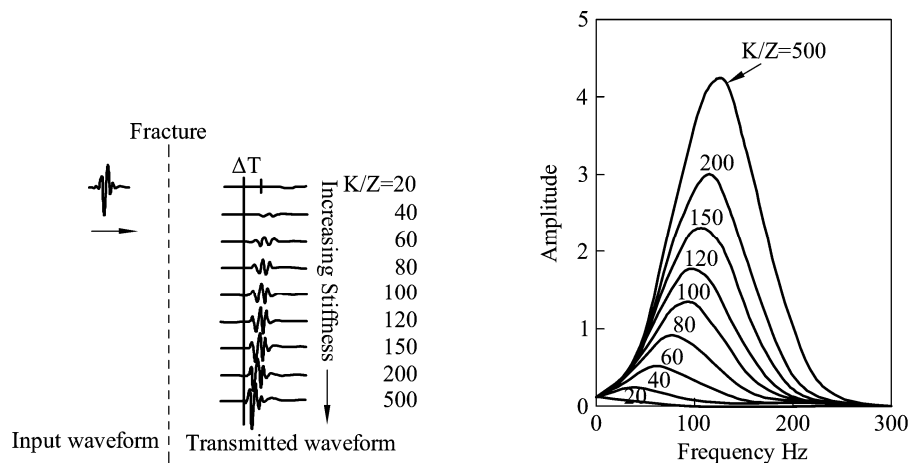


Figure 2.11. Illustration of the effects of a single fracture on the transmitted waveform and corresponding amplitude spectra (after Myer et al., 1990)

2.3.2.2 Joint dynamic shear strength

When a wave goes through a joint and the shear stress at the joint exceeds the joint shear strength, the joint will fail in shear and energy dissipation will occur. The joint shear strength under dynamic loads is affected by more factors than static strength. Only limited studies on it have been conducted. Two dynamic shear strength models of joints have been proposed; one is under cyclic load and the other under dynamic load with high loading rate.

Interlock/Friction Model

Cyclic experimental tests show that an offset phenomenon presents between the loading and unloading process (Jing *et al.* 1992 & 1993; Huang *et al.* 1993; Qiu *et al.* 1993; Kaña *et al.* 1996). The offset is recognised as an increase in shear stress required for shear displacement away from the natural rock alignment and a decrease in shear stress with displacement toward the naturally aligned rock position. Kaña *et al.* (1996) proposed an interlock/friction model by combining interlock function and friction function together

$$\tau = \sigma_n [f(x) + g(x)] \quad (2.24)$$

where $f(x)$ is the interlock function representing the offset; $g(x)$ is the friction function based on a combination of the approximate Coulomb law.

Jing *et al.* (1992 & 1993) found that the shear stress after the reverse of shear direction is almost constant and its magnitude is usually smaller than the residual shear stress during forward shear. They explained this phenomenon as due to different damage states of asperities. The asperities on a joint surface are classified into the primary asperities and higher order asperities. The higher order asperities are sheared off during forward shear and become negligible at reversal shear.

Frictional Sliding Model

When the loading rate is very high, the time and rate effects cannot be neglected when the sliding occurs along the joint surface. The frictional sliding model is used to model the frictional sliding behavior including unstable or stick-slip behavior under dynamic loading. Dieterich (1978; 1979a;

1979b and 1981) and Ruina (1980 &1983) conducted experiments on the friction sliding of rock joints and found that the shear strength at constant normal stress σ_n is dependent on the slip velocity V and state variables θ_i that represent the prior slip history. The general form of the relation is given as

$$\tau = F(V, \sigma_n, \theta_1, \theta_2, \dots, \theta_m) \quad (2.25)$$

The prior slip history in the form of dependence on a set of state variables evolves with on-going slip.

$$\frac{d\theta_i}{dt} = G_i(V, \sigma_n, \theta_1, \theta_2, \dots, \theta_m), \quad i=1, 2, \dots, m \quad (2.26)$$

A one-state variable constitutive relation was proposed by Ruina (1980 &1983) and expressed as

$$\tau = F(V, \theta) = \tau_* + \theta + a \ln(V/V_*) \quad (2.27)$$

$$d\theta/dt = G(V, \theta) = -(V/d)[\theta + b \ln(V/V_*)] \quad (2.28)$$

where V_* is a reference velocity at which $\tau = \tau_*$; a , b and d are positive empirical constants with units of stress, stress and length, respectively.

A two-state variable constitutive relation, which provides a close description of the observed behavior from experiments, was proposed by Ruina (1980 &1983) and expressed as

$$\tau = F(V, \theta_1, \theta_2) = \tau_* + \theta_1 + \theta_2 + a \ln(V/V_*) \quad (2.29)$$

$$d\theta_1/dt = G_1(V, \theta_1, \theta_2) = -(V/d_1)[\theta_1 + b_1 \ln(V/V_*)] \quad (2.30)$$

$$d\theta_2/dt = G_2(V, \theta_1, \theta_2) = -(V/d_2)[\theta_2 + b_2 \ln(V/V_*)] \quad (2.31)$$

Where τ_* , a , b_1 , b_2 , d_1 and d_2 are constants. Both one-state and two-state variable constitutive relations have been incorporated in the discrete element code UDEC which are verified by comparing numerical results for a single degree of freedom system with analytical results (Lorig and Hobbs 1990; Hobbs *et al.* 1990). It should be noted that this model is practically useful only if a reference velocity is defined. This may require estimation of a steady-state creep velocity for a fault as the reference condition, but very few publications are presented in this area.

2.3.3 Rock mass response

The natural rock masses that waves go through are often a composition of rock material and joints. The response of the rock masses is related to that of both rock material and joints. A wave going through rock material encounters material damping and geometric damping. When the wave hits a joint, the wave will be partially transmitted, reflected and lose some energy. For rock masses with several joint sets, multiple wave reflections occur. The superposition and interaction of waves including wave transmission and reflection between the joints cause very complicated wave propagation in jointed rock masses. In general, the poorer rock and rock masses with more joints cause more wave attenuation (Cook 1992).

